European Journal of Control (2011)3:222–236

DOI:10.3166/EJC.17.222–236

European Journal of Control

Minimum-Variance Control for Astronomical Adaptive Optics with Resonant Deformable Mirrors

Carlos Correia[1,2,*], Henri-François Raynaud[2], Caroline Kulcsár[2], Jean-Marc Conan[1]

[1] ONERA, DOTA, HRA unit, 92322 Chatillon, France;
[2] L2TI laboratory, University Paris 13, 93430 Villetaneuse, France

Adaptive Optics (AO) systems use a Deformable Mirror (DM) to counter in real-time the nefarious effects of atmospheric turbulence on ground-based telescope imaging. This article presents a brief historical overview of AO design, seen as a strongly multi-variable Minimum-Variance (MV) disturbance rejection problem associated with a hybrid continuous/discrete time MV control problem. It is shown that for a wide class of LTI DM and turbulence models, this hybrid MV problem can be transformed into an equivalent discrete-time LQG formulation. A discrete-time stochastic model enables to compute the optimal control in standard reconstructed feedback form and to evaluate performance degradation for simpler sub-optimal solutions. An example of tip-tilt DM control for the European Extremely Large Telescope (E-ELT) is presented.

Keywords: Minimum-variance stochastic control, LQG control, astronomical adaptive optics, extremely large telescopes

1. Introduction to Adaptive Optics Systems

Atmospheric turbulence is a major factor limiting performance of ground-based telescopes [27, 15]. It induces high-frequency erratic fluctuations in both intensity and shape of incoming light wave-fronts. Astronomical imaging devices, which integrate the flow of light over long exposure times, are grievously affected by fluctuations in wave-front shape. This results in a particularly nasty blurring effect, which unlike usual instrument-induced distortions can be corrected only to a limited extent by image post-processing. The obvious alternative is to seek to counter the effects of turbulence during the very process of image formation.

1.1. AO System Description

Counter turbulence effects can be achieved by deploying an adaptive optics (AO) system, whose basic set-up is presented in Fig. 1: the light gathered by the telescope bounces off a deformable mirror (DM), the shape of which is adjusted in real-time using measurements of the resulting corrected wave-front provided by a wave-front sensor (WFS). The turbulence and DM-induced deformations at time t are denoted respectively as $\phi^{\text{tur}}(t)$ and $\phi^{\text{cor}}(t)$, while

$$\phi^{\text{res}}(t) \triangleq \phi^{\text{tur}}(t) - \phi^{\text{cor}}(t), \tag{1}$$

is the residual deformation affecting image formation. In standard AO systems, the 'phase' variables ϕ^{tur}, ϕ^{cor} and ϕ^{res} are actually time-varying surfaces defined on the telescope's pupil.

In practice, they shall be represented as finite, albeit large-dimensional vectors on a suitable truncated basis of orthonormal generating two-dimensional functions. Fig. 2

*Correspondence to: C. Correia, E-mail: carlos.correia@nrc-cnrc.gc.ca

Received 13 January 2010; Accepted 26 January 2011
Recommended by E. Mosca, D.W. Clarke

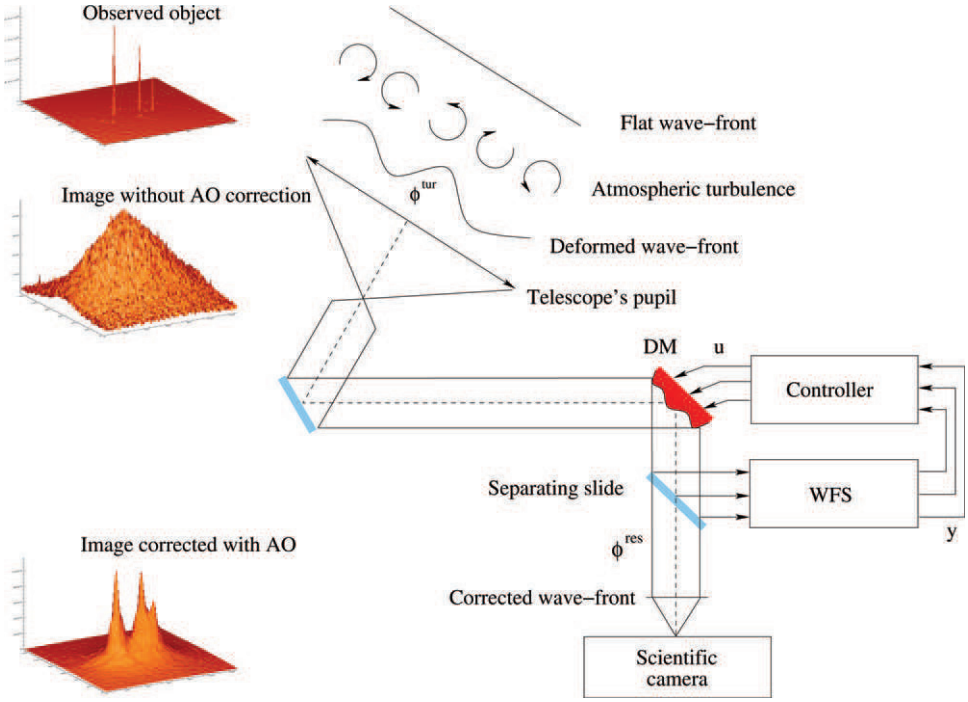

Fig. 1. Illustration of the AO principle. Diffraction-limited images are restored by real-time AO systems, in which a wave-front sensor (WFS) measures and a deformable mirror (DM) corrects in real-time for the distortions undergone by wave-fronts propagating through atmosphere. This single-conjugated AO configuration features a single DM and a single WFS.

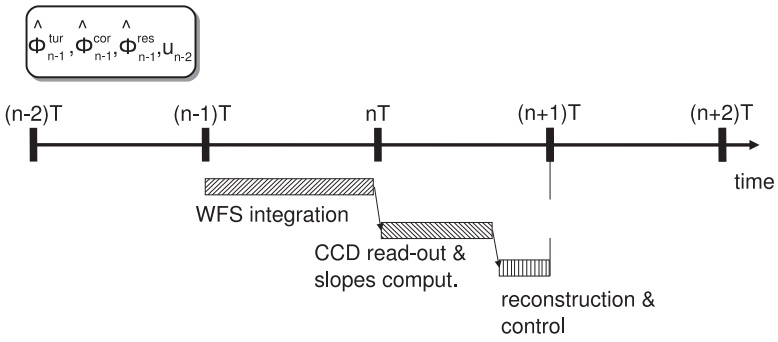

Fig. 2. Simplified temporal diagram of operations in AO. Controls u_n are applied at $t = nT_s$ over the interval $t \in [nT_s, (n+1)T_s]$. Any other sources of delay are neglected to have a total delay of two frames. Example: light is integrated from $t \in [(n-2)T_s, (n-1)T_s]$. From $t = (n-1)T_s$ onwards the detector is read-out and measurements computed. Wave-front reconstruction and control take place altogether in the same time slot at the end of which the controls u_n are ready for application and kept constant by a zero-order-hold through $t \in [nT_s, (n+1)T_s]$. Therefore this is said to be a two-frame delay system.

explains the temporal arrangement of operations and the delays incurred in AO.

1.2. Classical AO Control

Let u be the vector of DM control voltages and y the vector of WFS measurements. Since controls do not affect the turbulent phase, the AO control design problem clearly boils down to a standard disturbance rejection problem. Throughout this paper, is will be assumed that the DM can be modelled as a continuous-time LTI system, while the WFS, which integrates the residual phase over successive exposure frames $[nT_s, (n+1)T_s]$, can be modelled as a discrete-time LTI system with sampling time T_s. It will also be assumed that u and y are applied/processed through the AO real-time computer with the same sampling interval T_s, with u_n, y_n denoting the control/measurement applied/registered at sampling time $t = nT_s$. It is assumed that the control u is applied through a zero-order hold, so that $u(t) = u(nT_s) = u_n$ for all $nT_s \leq t < (n+1)T_s$.

The early ideas of Babcock to build an AO system date back from the 1950's. However, the era of

astronomical AO opened a few decades later in 1990, with the COME-ON experiment on an European Southern Observatory's (ESO) telescope [28]. Nowadays AO systems are routinely utilised on most large telescopes, such as ESO's VLT, Gemini's North and South, Keck's and Subaru's to cite a few.

All currently operational systems rely on a simple 'standard' AO control structure, namely a static decoupling matrix and a series of pure integral scalar controllers [9, 12]. Yet AO loops are strongly multi-variable systems – u, y and ϕ^{tur} are vectors with at least several dozens coordinates, soon to increase to several hundreds or even thousands. Furthermore, those variables evolve in distinct physical spaces, whose dimensions do not match. All this suggests that much is to be gained by switching to a state-space approach.

1.3. Strehl-Optimising AO Control – A Brief Overview

A relevant AO performance criterion to be minimised is the variance of the continuous-time-valued residual phase, defined as

$$J^{\text{c}}(u) \triangleq \lim_{T_f \to +\infty} \frac{1}{T_f} \int_0^{T_f} \left\| \phi^{\text{res}}(t) \right\|^2 dt. \tag{2}$$

This is so since the Strehl-ratio (the ratio of the maximum of the point-spread function (PSF) of the distorted image divided by the maximum of the theoretical diffraction-limited image PSF) is hence maximised [13].

For this class of minimum-variance problems, LQG techniques appear particularly attractive: minimum-variance (MV) control makes perfect applicative sense in AO given the quadratic nature of the minimisation cost functional. Furthermore, readily available LQ solvers handle reasonably comfortably large dimension optimisation problems.

In the last 20 years or so, several attempts to formulate the AO disturbance-rejection problem in the scope of the LQG framework have been pursued, the first contributions being those of [22, 23, 30] and, more recently, using a H_2 framework [14]. In this contribution the mixed continuous-time/discrete-time nature of AO systems is fully considered leading to different versions of the optimisation criterion, overcoming sub-optimal controller design and possibly degraded performance.

When the DM's transient response is negligible compared with the sampling interval T_s, its dynamics can be reduced to its DC gain matrix N (the so-called 'DM influence matrix', a concatenation of the DM local surface deformations at every actuator location). Then $\phi^{\text{cor}}(t) = Nu_n \forall nT_s \leq t < (n+1)T_s$ and it is shown in [18, 17] that the globally optimal MV control for a DM with infinitely fast response controlled via a zero-order hold (ZOH) – that is, the discrete control minimising the continuous-time criterion J^{c} in Eq. (2) – is obtained by minimising the equivalent discrete MV criterion involving only average-sampled values

$$J^{\text{d}}(u) \triangleq \lim_{M \to +\infty} \frac{1}{M} \sum_{n=0}^{M-1} \left\| \overline{\phi}^{\text{tur}}_{n+1} - Nu_n \right\|^2, \tag{3}$$

where $\overline{\phi}^{\text{tur}}_{n+1}$ is the temporal average of the turbulent phase over $[nT_s, (n+1)T_s]$, *i.e.*

$$\begin{aligned} \overline{\phi}^{\text{tur}}_{n+1} &\triangleq \frac{1}{T_s} \int_{nT_s}^{(n+1)T_s} \phi^{\text{tur}}(t)\, dt \\ &= \frac{1}{T_s} \int_0^{T_s} \phi^{\text{tur}}(nT_s + t)\, dt. \end{aligned} \tag{4}$$

As a direct corollary, when $\overline{\phi}^{\text{tur}}$ can be modelled as the output of a stochastic LTI system, the MV controller is obtained as the solution of a standard discrete LQG problem, *i.e.* in reconstructed feedback form using Kalman filtering [1]. This approach has been validated on AO test benches and extended to more complex multi-conjugate AO configurations [24, 8]. Off-line and real-time computational issues for systems with very large number of actuators/measurements were addressed in [4].

In recent articles, D.P. Looze has investigated the same MV control problem, starting from the assumption that ϕ^{tur} can be modelled as the output of a continuous-time stochastic LTI system, and applying standard lifting methods from sampled-data theory [19, 20]. The particular structure of this hybrid disturbance-rejection problem, and especially the fact that the plant to be controlled is the combination of a stochastic disturbance model and of a deterministic actuator model is not fully exploited.

In this paper, a different approach is used where the equivalent discrete-time criterion is derived directly from the interaction between the DM's dynamics and the continuous-time quadratic criterion, *i.e.* without any particular assumption on the turbulence. The turbulence model is then required only at a later stage, to solve the equivalent discrete LQG problem.

These different starting points provide different insights. From a control-theoretical point-of-view, the approach in this paper translates into a different definition of the 'full information' assumption for the turbulent part of the system (disturbance model), a key issue in a state-space framework. More precisely, in [19, 20] the full information assumption means that the value of the turbulence model's internal state is known at the time index when the control is to be computed. In this paper, the full information assumption means that at time nT_s *future* values of the turbulence trajectory are known, up

to time $(n+1)T_s$. In an LQG framework, this obviously results in a different balance between the full information optimal control problem and the minimum-variance estimation/prediction problem. Thus, in the simple but important case where the DM's dynamics are reduced to pure delays, the full information optimal control problem can be solved by a straightforward orthogonal projection, whereas the approach in [19, 20] requires solving a control algebraic Riccati equation (ARE). Also, no proof is included that in the absence of additional penalty on the control energy, the discrete-time criterion is guaranteed to result in a non-singular LQ problem, with a unique solution.

The astronomical community is currently assisting to tremendous advancements in telescope capabilities. Though for current generation telescopes (below 10 m diameter) AO systems utilise DM whose bandwidths are well above the sampling frequency a new generation is underway. The planned designs include physically large DM likely to exhibit significantly lower resonance frequencies, possibly associated with poorly damped modes. Synthesis of controllers that account for DM dynamics is motivated by recent projects of secondary deformables for the Extremely Large Telescopes (ELT). Furthermore, it comes along with the stance of corrections to within a few fold the telescope's diffraction-limit. Resolving to study the MV problem for the non-rigid DM has become a clearly identified area where progress is to be made.

The optimal approach is to derive the hybrid MV criterion by directly assessing the effect of control decisions on the value of J^{c} in Eq. (6) . In [6, 7], it was shown that a completely equivalent and well-posed MV criterion can be constructed in this way for a wide class of continuous-time DM LTI dynamics, and independently of any particular assumption on the turbulent phase.

This paper intends to fully exploit the particular structure of this hybrid disturbance-rejection problem, and especially the fact that the plant to be controlled is the combination of a stochastic disturbance model and of a deterministic actuator model. It is shown that in the general case, the equivalent discrete-time LQ criterion, in addition to $\overline{\phi}^{\mathrm{tur}}$, shall involve the DM's internal state and another, more complicated, weighted temporal average of the turbulent phase. In addition, the resulting discrete-time model also enables to evaluate J^{c} for any sub-optimal choice of observer and feedback gains – a class of controllers which includes the optimal solution in the infinitely-fast DM case. One can thus quantify precisely the degradation in performance resulting from using this simpler solution *in lieu* of the optimal one. From now on it is dubbed 'sub-optimal'.

Finally, note that the time-line for real-time AO control presented in Fig. 2, where a whole DM/WFS frame is allocated for measurement processing and control calculation, may induce performance degradation when these operations take only a fraction of one WFS frame. For the sake of simplicity, only the case where DM and WFS operations are synchronised is presented here. However, this is not an inherent limitation of the approach, which can be extended to the case where the WFS and DM operate in asynchronous mode [25] and possibly at different frame-rates [16].

Using the approach outlined in [6], this paper extends these results to a fairly general class of continuous-time DM with non-negligible dynamics. Special emphasis is put on using a particularly suited modal control expressed as a truncated sum of the Zernike polynomials and its connections to the DM mechanical eigenmodes vectorial space. An all-modes controller is proposed integrating infinitely fast with slower modes in a common controller.

An illustrative application to the control of two-degrees of freedom tip-tilt platform for the European Extremely Large Telescope (E-ELT) is presented.

The controller behaviour with respect to the DM natural resonant frequency and damping coefficient extends earlier results found in [7].

2. LQG Control for Adaptive Optics

2.1. Infinitely Fast Deformable Mirrors

This section briefly recalls the solution of the MV AO control problem in the infinitely fast DM case, which has been established in [17, 18].

With no loss of generality, it shall be assumed that the DM influence matrix N is full column rank, in other words that $N^{\mathrm{T}}N$ is invertible. Breaking down the performance criterion in sample period-sized slabs, J^{c} can be written as

$$J^{\mathrm{c}}(u) = \lim_{M\to+\infty} \frac{1}{M} \sum_{n=0}^{M-1} j_n^{\mathrm{c}}(u), \tag{5}$$

with

$$j_n^{\mathrm{c}}(u) \triangleq \frac{1}{T_s} \int_{nT_s}^{(n+1)T_s} \left\| \phi^{\mathrm{res}}(t) \right\|^2 dt. \tag{6}$$

As noted above, the infinitely fast DM assumption results in $\phi^{\mathrm{cor}}(t) = Nu_n$ for $t \in [nT_s, (n+1)T_s]$, so that, using Eq. (1) and Eq. (6) it comes

$$j_n^{\mathrm{c}}(u) = \frac{1}{T_s} \int_{nT_s}^{(n+1)T_s} \left\| \phi^{\mathrm{tur}}(t) \right\|^2 dt - 2u_n^{\mathrm{T}} N^{\mathrm{T}} \overline{\phi}_{n+1}^{\mathrm{tur}} + u_n^{\mathrm{T}} N^{\mathrm{T}} N u_n. \tag{7}$$

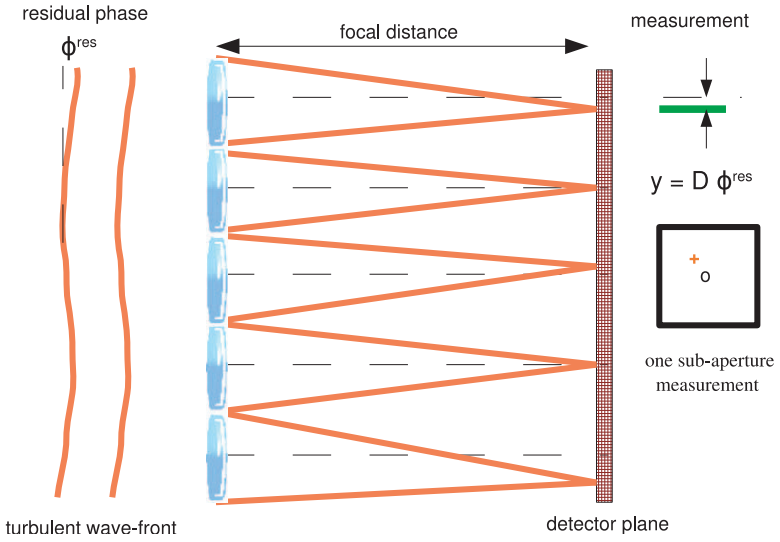

Fig. 3. Hartmann-Shack wave-front sensor. The xy tilted wave-front at the entrance of the pupil-plane forms a displaced image with respect to the reference plane wave-front. The bi-dimensional displacement is linked to the wave-front's average local angle-of-arrival over each sub-aperture, and thus to the wave-front gradient.

Take:

$$j_n^{\mathrm{d}}(u) \triangleq \left\| \overline{\phi}_{n+1}^{\mathrm{tur}} - Nu_n \right\|^2, \\ = \left\| \overline{\phi}_{n+1}^{\mathrm{tur}} \right\|^2 - 2u_n^{\mathrm{T}} N^{\mathrm{T}} \overline{\phi}_{n+1}^{\mathrm{tur}} + u_n^{\mathrm{T}} N^{\mathrm{T}} N u_n, \quad (8)$$

and define

$$J^{\mathrm{d}}(u) \triangleq \lim_{M\to+\infty} \frac{1}{M} \sum_{n=0}^{M-1} j_n^{\mathrm{d}}(u). \quad (9)$$

Because j_n^{d} is derived from j_n^{c} by adding/subtracting terms independent of u, it is obvious that $\arg\min J^{\mathrm{d}} = \arg\min J^{\mathrm{c}}$. And since there is no DM dynamics, this equivalent discrete LQG problem is readily solved using *certainty equivalence*. The solution of this equivalent discrete-time LQG problem is solved by projecting the average turbulent phase over the next sampling period onto the DM's space $Im(N)$. The full-information MV control is thus

$$u_n^{\mathrm{fi}} = \left(N^{\mathrm{T}} N\right)^{-1} N^{\mathrm{T}} \overline{\phi}_{n+1}^{\mathrm{tur}}. \quad (10)$$

Two interesting features of the full information control are worth noting: (1) it does not depend on any particular assumption on the turbulent phase; (2) it effectively redefines 'full information' as the advance knowledge not of the whole turbulent phase trajectory over the next sampling interval, but rather of its average value. The latter is specially interesting since WFS measurements can also be expressed as functions of $\overline{\phi}^{\mathrm{tur}}$. More precisely, commonly used WFS devices, such as the Hartmann-Shack (HS), rely on an array of sub-apertures placed on a 2-D grid, which temporally integrate the light flux emanating from a guide star to provide a measurement of the local spatial gradient of the phase – see Fig. 3. The whole wave-front shape is reconstructed from measurements using inverse problem theory [10]. Assuming a linear response, their output can be modelled in the first approximation as

$$y_n = D\overline{\phi}_{n-1}^{\mathrm{res}} + w_n, \quad (11)$$

where D is the phase-to-WFS operator that relates wave-front to its average phase gradients in every sub-aperture. The measurement noise w is assumed to be a Gaussian white noise sequence independent of ϕ^{tur}. For an infinitely fast DM, this measurement equation can be rewritten as (refer to Fig. 2)

$$y_n = D\overline{\phi}_{n-1}^{\mathrm{tur}} - DNu_{n-2} + w_n. \quad (12)$$

As a consequence, *any* stochastic model of $\overline{\phi}^{\mathrm{tur}}$ will enable to construct an 'exhaustive control-oriented' model for the AO loop, *i.e.* one from which the globally optimal MV control can be derived using standard LQG procedures.

Hence, assuming that $\overline{\phi}^{\mathrm{tur}}$ is a stochastic Hilbertian process, the MV control in incomplete information becomes

$$u_n^{ii} = \left(N^{\mathrm{T}} N\right)^{-1} N^{\mathrm{T}} \widehat{\overline{\phi}}_{n+1|n}^{\mathrm{tur}}, \quad (13)$$

where $\widehat{\overline{\phi}}_{n+1|n}^{\mathrm{tur}}$ is the MV estimator of $\overline{\phi}_{n+1}^{\mathrm{tur}}$ given all information available at time $t = nT_s$ – in other words, the conditional expectation of $\overline{\phi}_{n+1}$ with respect to statistical priors and measurements $y_0, \ldots, y_n$. In practice, this

optimal predictor is computed as the output of a Kalman filter [1].

2.2. General Case: DM with LTI Dynamics

Proposition 1: *Assume that the DM-generated correction phase is* $\phi^{cor}(t) = Np(t)$ *and that the DM surface is related to u through a state-space model in the form*

$$\dot{x}^m(t) = A_m x^m(t) + B_m u(t) \tag{14a}$$

$$p(t) = C_m x^m(t) + D_m u(t) \tag{14b}$$

$$\phi^{cor}(t) = Np(t), \tag{14c}$$

where (i) A_m *is a Hurwitz matrix; (ii) the pair* (A_m, C_m) *is observable; (iii) the DC gain between u and p is unitary.*

Let J^c *be defined as in (2). Then*

$$\arg\min_{\mathcal{U}} J^c = \arg\min_{\mathcal{U}} J^d, \tag{15}$$

where

$$J^d(u) \triangleq \lim_{M\to+\infty} \frac{1}{M} \sum_{n=0}^{M-1} \left(z_n^T Q_2 z_n + 2 z_n^T S_1 u_n + u_n^T R_1 u_n \right), \tag{16}$$

with

$$z_n \triangleq \begin{pmatrix} \overline{\phi}^{tur}_{n+1} \\ \overline{\varphi}^{tur}_{n+1} \\ x_n^m \end{pmatrix} \triangleq \begin{pmatrix} \dfrac{1}{T_s}\displaystyle\int_0^{T_s} \phi^{tur}(nT_s + s)\, ds \\ \dfrac{1}{T_s}\displaystyle\int_0^{T_s} e^{sA_m^T} C_m^T N^T \phi^{tur}(nT_s + s)\, ds \\ x^m(nT_s) \end{pmatrix}. \tag{17}$$

$$Q_2 \triangleq \begin{pmatrix} 2\kappa N N^T & 0 & 0 \\ 0 & \kappa\left(I + 2A_m^{-1} B_m B_m^T A_m^{-T}\right) & -I \\ 0 & -I & Q_0 \end{pmatrix}. \tag{18}$$

$$S_1^T \triangleq \begin{pmatrix} -N^T & -B_m^T A_m^{-T} & S_0^T \end{pmatrix}. \tag{19}$$

$$R_1 \triangleq \frac{1}{T_s}\int_0^{T_s} \left(I + C_m e^{sA_m} A_m^{-1} B_m\right)^T N^T N \times \left(I + C_m e^{sA_m} A_m^{-1} B_m\right) ds, \tag{20}$$

$$S_0 \triangleq \frac{1}{T_s}\int_0^{T_s} e^{sA_m^T} C_m^T N^T N \left(I + C_m e^{sA_m} A_m^{-1} B_m\right) ds, \tag{21}$$

$$Q_0 \triangleq \frac{1}{T_s}\int_0^{T_s} e^{sA_m^T} C_m^T N^T N C_m e^{sA_m} ds, \tag{22}$$

where $\kappa > 0$ *is an arbitrary constant. In addition, for large enough values of* κ*,*

$$P \triangleq \begin{pmatrix} Q_2 & S_1 \\ S_1^T & R_1 \end{pmatrix} \geq 0 \quad \textit{and} \quad R_1 > 0. \tag{23}$$

Proof. Since $u(t) = u_n \forall t \in [nT_s, (n+1)T_s]$, the solution of the first equation in (14) is given by

$$p(t) = C_m e^{(t-nT_s)A_m} x_n^m + \left(\int_0^{t-nT_s} C_m e^{vA_m} B_m dv + D_m \right) u_n. \tag{24}$$

Following the same approach as in the instantaneous response case, step one is to insert the expression of $p(t)$ into $j_n^c(u)$ and to turn it into a quadratic function of u_n similar to (7), which can be expressed in fairly compact form by evaluating several matrix exponential integrals. Step two is to add/subtract terms independent of u so as to obtain a one-frame slab of a positive-definite function of (z_n, u_n). Details of this construction are provided in Appendix.

Remarks:

(i) Proposition 1 can be viewed as a natural extension of the design procedure in Section 2.1 for the infinitely fast case. Conversely, the infinitely fast DM case is recovered as a limit case of Proposition 1. To prove it, consider a set of DM models in the form (14) depending on a parameter θ such that for $\theta \to 0$, the maximum value of the real part of all eigenvalues of A_{m} tends to $-\infty$, so that the dynamics, loosely speaking, become 'infinitely fast'. The corresponding asymptotic behaviour for the weighting matrices in Proposition 1 is therefore

$$\lim_{\theta\to 0} Q_0 = 0, \quad \lim_{\theta\to 0} S_0 = 0, \quad \lim_{\theta\to 0} R_1 = N^{\mathrm{T}} N. \tag{25}$$

Assuming that ϕ^{tur} is a stationary process with finite variance, then $\bar{\varphi}^{\mathsf{tur}}$ also converges towards zero in a stochastic L_2 sense, with both its mean and variance converging towards zero. Thus, in the limit case, one may remove both x_n^m and $\bar{\varphi}^{\mathsf{tur}}$ from z. Taking $\kappa = 1$, this results in the same discrete criterion as in Section 2.1.

(ii) From a control-theoretical point of view $\bar{\varphi}^{\mathsf{tur}}$, defined in (17), corresponding to the average DM impulse response weighted phase over T_s, can be interpreted as a dual control variable, since it formally derives from manipulations of the scalar product $\langle \phi, \psi \rangle = \int_0^{T_s} \phi(t)^{\mathrm{T}} \psi(t) dt$, with ϕ, ψ arbitrary phase vectors.

The formulae defining $\bar{\varphi}^{\mathsf{tur}}$ correspond to convolution integrals in retrograde time. In order to express them as the output of a causal system, as will be done in the next section, it will therefore be necessary to reverse time once more and to include in

the process appropriate anti-causal (and unstable) operators.

(iii) Taken together, the properties $R_1 > 0$ and $P \geq 0$ for large enough values of κ ensure that the corresponding LQ problem is non-singular. Because the values of the κ-dependent terms in J^{d} are not affected by the control u, this also guarantees that the discrete-time LQ problem remains non-singular for *all* values of κ, including $\kappa = 0$. In practice, this means that when z_n is the output of a discrete-time LTI system with control input u, the MV control problem can be constructively solved using standard control software, e.g. Matlab (with either $\kappa > 0$ or $\kappa = 0$, depending on the said solver's constraints), yielding a unique MV control sequence in usual state-feedback form. The optimal value of the original continuous-time criterion J_c can then be computed by setting $\kappa = 0$, as shown in Appendix B.

2.3. Control-Oriented Model

As an immediate corollary of Proposition 1, the globally optimal MV control minimising the continuous-time criterion J^{c} can be computed from any stochastic state-space model able to produce as output both performance variable z and measurement y. Substituting the expression for $p(t)$ in (24) into the measurement equation (11), and evaluating the resulting matrix exponential integrals results in

$$y_n = D\bar{\phi}^{\mathsf{tur}}_{n-1} - DN\frac{C_m}{T_s}\left(e^{T_s A_m} - I\right)A_m^{-1}x^m_{n-2} + DN\left(\frac{C_m}{T_s}\left(e^{T_s A_m} - I\right)A_m^{-2}B_m + I\right)u_{n-2} + w_n. \tag{26}$$

The following proposition enables to construct such a 'control-oriented' model from essentially any combination of LTI turbulence and DM models:

Proposition 2: *Suppose the measurement and DM models of (26) and (14), and a further stochastic turbulence model in the general form*

$$dx_\phi(t) = A_\phi x_\phi(t)\, dt + d\eta \tag{27a}$$

$$\phi^{tur}(t) = C_\phi x_\phi(t), \tag{27b}$$

where A_ϕ is a Hurwitz matrix (so that x_ϕ, ϕ^{tur} are stationary processes) and η is a (continuous-time) Gaussian white noise with power-spectral density (PSD) Σ_η, independent from the measurement noise w.

Let z_n be defined by (17) and y_n by (11). Then there exists a discrete Gaussian white noise v independent of w with variance Σ_v such that

$$x_{n+1} = Ax_n + Bu_n + \Gamma v_n \tag{28a}$$

$$y_n = Cx_{n-1} + w_n \tag{28b}$$

$$z_n = Gx_n \tag{28c}$$

with

$$x_n \triangleq \begin{pmatrix} x_{\phi,n+1} \\ \overline{\phi}^{tur}_{n+1} \\ \overline{\varphi}^{tur}_{n+1} \\ \overline{\phi}^{tur}_{n} \\ x^m_n \\ x^m_{n-1} \\ u_{n-1} \end{pmatrix}, \tag{29}$$

$$A \triangleq \begin{pmatrix} e^{T_s A_\phi} & 0 & 0 & 0 & 0 & 0 & 0 \\ M_1 & 0 & 0 & 0 & 0 & 0 & 0 \\ M_2 & 0 & 0 & 0 & 0 & 0 & 0 \\ 0 & I & 0 & 0 & 0 & 0 & 0 \\ 0 & 0 & 0 & 0 & e^{T_s A_m} & 0 & 0 \\ 0 & 0 & 0 & 0 & I & 0 & 0 \\ 0 & 0 & 0 & 0 & 0 & 0 & 0 \end{pmatrix}, \tag{30}$$

$$B \triangleq \begin{pmatrix} 0 & 0 & 0 & 0 & B_m^T(e^{T_s A_m^T} - I)A_m^{-T} & 0 & I \end{pmatrix}^T, \tag{31}$$

$$\Gamma \triangleq \begin{pmatrix} I & 0 & 0 \\ 0 & I & 0 \\ 0 & 0 & I \\ 0 & 0 & 0 \\ 0 & 0 & 0 \\ 0 & 0 & 0 \\ 0 & 0 & 0 \end{pmatrix}, \qquad G \triangleq \begin{pmatrix} 0 & 0 & 0 \\ I & 0 & 0 \\ 0 & I & 0 \\ 0 & 0 & 0 \\ 0 & 0 & I \\ 0 & 0 & 0 \\ 0 & 0 & 0 \end{pmatrix}^T, \tag{32}$$

$$C \triangleq \begin{pmatrix} 0 & 0 & 0 & D & 0 & -\frac{1}{T_s}DNC_m\left(e^{T_s A_m} - I\right)A_m^{-1}\cdots - DN\left(I + \frac{1}{T_s}C_m\left(e^{T_s A_m} - I\right)A_m^{-2}B_m\right)\end{pmatrix}, \tag{33}$$

$$M_1 \triangleq \begin{pmatrix} 0 & I & 0 \end{pmatrix} e^{T_s A_c} \begin{pmatrix} I & 0 & 0 \end{pmatrix}^T, \tag{34}$$

$$M_2 \triangleq \begin{pmatrix} 0 & 0 & I \end{pmatrix} e^{T_s A_c} \begin{pmatrix} I & 0 & 0 \end{pmatrix}^T, \tag{35}$$

$$\Sigma_v \triangleq \int_0^{T_s} e^{sA_c} \begin{pmatrix} I & 0 & 0 \end{pmatrix} \Sigma_\eta \begin{pmatrix} I & 0 & 0 \end{pmatrix}^T e^{sA_c^T} ds, \tag{36}$$

where

$$A_c \triangleq \begin{pmatrix} A_\phi & 0 & 0 \\ \frac{1}{T_s} C_\phi & 0 & 0 \\ \frac{1}{T_s} C_m^T N^T C_\phi & 0 & -A_m^T \end{pmatrix}. \tag{37}$$

Refer to [7] for a complete proof of Proposition 2.

2.4. Real-Time Operation

In this model, the measurement y_n depends on x_{n-1} instead of x_n, as customary. This non-standard measurement equation allows for a more compact state-space representation and real-time implementation of the control in standard reconstructed feedback form. As we shall see, this effectively transforms the recursive equation for the estimator form of the Kalman filter in a more compact predictor (observer) form. This is formally achieved by substituting the conditional expectations related to $\mathcal{Y}_{n-1} = (y_{n-1}, \ldots, y_0)$ by $\mathcal{Q}_n = (q_n, \ldots, q_0) = \mathcal{Y}_{n-1}$, *i.e.* a new set of 1-step ahead pseudo-measurements $q_n = Cx_n + w'_n \equiv y_{n+1}$. The following operations are implemented in real-time:

$$\widehat{y}_{n|\mathcal{Y}_{n-1}} = C\widehat{x}_{n-1|\mathcal{Y}_{n-1}}, \tag{38a}$$

$$\widehat{x}_{n|\mathcal{Y}_n} = A\widehat{x}_{n-1|\mathcal{Y}_{n-1}} + Bu_{n-1} + L_\infty \left(y_n - \widehat{y}_{n|\mathcal{Y}_{n-1}}\right), \tag{38b}$$

$$u_n = K_\infty \widehat{x}_{n|\mathcal{Y}_n}, \tag{38c}$$

where the first line stands for the estimated measurement from model, the second for the filter update and prediction and the third for the optimal control step. Appendix B further explains this indexing choice.

The asymptotic versions of the observer gain L_∞ and control gain K_∞ are used under the stationary hypothesis. This is so since AO performance is measured in terms of long-exposure Strehl-ratio [27, 15]. Therefore, using the asymptotic version does not introduce any loss when looking at the infinite-horizon performance. Both these gains are computed from Algebraic Riccati Equations for both the optimal estimation and the optimal control steps.

In Eq. (38b), two occurrences of the DM state (x_n^m and x_{n-1}^m), together with the delayed control u_{n-2}, are included in $\widehat{x}_{n-1|\mathcal{Y}_{n-1}}$. However, since all three are deterministic variables, the corresponding components of the Kalman gain are zero. In other words, these parts of the Kalman filter are simply carbon copies of their deterministic dynamics. Thus, in real-time computation, they can be efficiently implemented as a copy of the discretised version of (14a) (to compute the estimate of x_n^m) and two delay lines (to compute the estimate of x_{n-1}^m and u_{n-2}).

3. Deformable Mirror Modelling

Future AO systems design for ELT use pre-focal deformable mirrors that have more than a thousand actuators [2, 26, 29]. Any control strategy to tackle the DM dynamics in such structures would naturally start by analysing the DM behaviour on the set of its eigenmodes. This is a crucial point for two main reasons: first, the overall dynamics cannot be easily derived from the individual dynamics of single isolated actuators and second, it allows to break down the regulator synthesis into a smaller set of modes whose dynamical behaviour must be taken into account on the regulator side. Mechanical eigenmodes that are temporally fast or that are spatially associated with low-energy turbulent modes can, as a first approximation, be considered infinitely fast. Therefore the results of Section 2.1 apply to these cases.

3.1. DM Modal Control

Equation (14) defines a very general class of DM's dynamics. One important special case is when the DM's response can be decomposed according to a set of independent mechanical eigenmodes. Assuming that the total number of eigenmodes retained in the model to be n_e, this would result in a relation of the form

$$\phi^{\mathsf{cor}}(t) = \sum_{j=1}^{n_e} v_j d_j(t) \tag{39}$$

where v_j is the jth DM surface eigenvector, and the scalar function $d_j(t)$ its amplitude at time t. Note that the number of DM's mechanical eigenmodes that needs to be retained in order to model its dynamics with sufficient accuracy is different from the number of 'turbulent modes' retained to model the phase variables, *i.e.* the dimension of the phase vectors ϕ^{tur} and ϕ^{cor}. To satisfy the assumptions in Proposition 1, it is necessary to assume that the subspace spanned by these DM's eigenmodes lies within the subspace spanned by the static DM's influence functions, so that $n_e \leq dim(u)$. Consider first the case where $n_e = dim(u)$, and assume that $V \triangleq \left(v_1 \cdots v_{n_e}\right)$ has full column rank $\dim(u)$. Let $e(t)$ denote the control action expressed in the basis of DM's eigenmodes, in other words the unique solution of $Ve(t) = Nu(t)$. Likewise, $p(t)$, which corresponds to the DM's instantaneous deformation expressed in the basis of influence functions, can be mapped into eigenmode coordinates through $Vd(t) = Np(t)$. These relations thus define a bijection between the input-output pairs (u, p) and (e, d). Assume now that the input-output model for each DM eigenmode is a simple second-order temporal response

with unitary DC gain, natural frequency ω_j and damping coefficient ξ_j:

$$\ddot{d}_j(t) + 2\xi_j\omega_j\dot{d}_j(t) + \omega_j^2 d_j(t) = \omega_j^2 e_j(t) \tag{40}$$

Then a simple state-space model for the dynamics between e_j and d_j is therefore

$$\dot{\vartheta}(t) = \begin{pmatrix} \dot{\vartheta}_1(t) \\ \dot{\vartheta}_2(t) \end{pmatrix} \tag{41}$$

$$= \begin{pmatrix} 0 & 1 \\ -\omega_j^2 & -2\xi_j\omega_j \end{pmatrix} \begin{pmatrix} \vartheta_1(t) \\ \vartheta_2(t) \end{pmatrix} + \begin{pmatrix} 0 \\ \omega_j^2 \end{pmatrix} e_j(t)$$

$$d_j(t) = \begin{pmatrix} 1 & 0 \end{pmatrix} \begin{pmatrix} \vartheta_1(t) \\ \vartheta_2(t) \end{pmatrix}. \tag{42}$$

Defining Ω as the diagonal matrix with general term ω_j and Ξ the diagonal matrix with general term ξ, this set of decoupled models can be concatenated into a single state-space model with input e, output d and state vector x_m:

$$\dot{x}_m(t) = \begin{pmatrix} 0 & I \\ -\Omega^2 & -2\Omega\Xi \end{pmatrix} x_m(t) + \begin{pmatrix} 0 \\ \Omega^2 \end{pmatrix} e(t) \tag{43}$$

$$d(t) = \begin{pmatrix} I & 0 \end{pmatrix} x_m(t) \tag{44}$$

For the system with input u and output p, this corresponds to a state-space model in the form of Eq. (14), with

$$A_m = \begin{pmatrix} 0 & I \\ -\Omega^2 & -2\Omega\Xi \end{pmatrix}, \tag{45a}$$

$$B_m = \begin{pmatrix} 0 \\ \Omega^2 \end{pmatrix} (V^{\mathrm{T}}V)^{-1}V^{\mathrm{T}}N, \tag{45b}$$

$$C_m = (N^{\mathrm{T}}N)^{-1}N^{\mathrm{T}}V \begin{pmatrix} I & 0 \end{pmatrix}, \tag{45c}$$

$$D_m = 0. \tag{45d}$$

A useful variant of this construction is derived by assuming that the DM's eigenmodes can be separated into slow modes with second-order dynamics and fast modes with instantaneous response. Let n_s, n_f be the numbers of slow and fast modes, let V be partitioned accordingly as $V = (V_s \quad V_f)$, and let Ω_s and Ξ_s be the diagonal matrices containing the slow modes' natural frequencies and damping coefficients. With this notation, it is immediately checked that the DM's state space model becomes

$$A_m = \begin{pmatrix} 0 & I \\ -\Omega_s^2 & -2\Omega_s\Xi_s \end{pmatrix}, \tag{46a}$$

$$B_m = \begin{pmatrix} 0 \\ \Omega_s^2 \end{pmatrix} \begin{pmatrix} I & 0 \end{pmatrix} (V^{\mathrm{T}}V)^{-1}V^{\mathrm{T}}N, \tag{46b}$$

$$C_m = (N^{\mathrm{T}}N)^{-1}N^{\mathrm{T}}V \begin{pmatrix} I & 0 \\ 0 & 0 \end{pmatrix}, \tag{46c}$$

$$D_m = (N^{\mathrm{T}}N)^{-1}N^{\mathrm{T}}V \begin{pmatrix} 0 \\ I \end{pmatrix} \tag{46d}$$

The application to tip-tilt mirror control presented in section 4 can be seen as a prototypical simple case of such eigenmode-based models.

4. Tip-Tilt Mirror Control for the E-ELT

In AO systems, the so-called tip-tilt modes correspond to the two degrees of freedom bending of a flat wave-front. These two modes can be corrected for, together with the other turbulent modes, by a DM with deformable surface. They can also be handled separately by a specialised tip-tilt mirror (TTM), which is essentially a mobile flat mirror (an equivalent alternative is to mount the DM on a two-degrees of freedom mobile tip-tilt platform). In practice, the use of a specialised tip-tilt actuator enables to 'off-load' a part of the control effort from the DM. For a given level of turbulence energy, this enables to use DMs with lower maximum stroke – or, conversely, to compensate effectively more energetic turbulence.

More recently, the migration from active to adaptive telescopes with the inclusion of DM in the optical path (see for example [2]) and the foreseen designs for the ELT employ structurally massive AOS affected by large disturbances induced by the telescope's mechanical vibrations [29]. Due to structure stiffness, low-order optical modes tend to be particularly affected by wind buffeting, thus emphasising the importance of accurate TT control. With no loss of generality, $p(t)$ is considered here as the equivalent on-sky angle of the TTM with the flat reference position, given in milliarcseconds (mas).

In addition, this set of modes has the following features:

(i) the greatest associated turbulent energy [21]; the down-scaled infinite element model provided by the European Southern Observatory [29] shows that this very behaviour is found on the mechanical side also;
(ii) TT modes are very easily computed from measurements by just averaging the Hartmann-Shack 'x' and 'y' local spatial derivatives;
(iii) TT modes are statistically decoupled from each other, both temporally and spatially. This suggests that decoupled modal control can be applied, thus simplifying the initial multi-mode problem.

Note that those 'on-sky angles' modes, while decoupled from one another, are not statistically independent from higher-order turbulent modes.

Still, the *full-information* controller derived here is indeed optimal, since the LQ solution is independent of any mode correlations – it does not depend on the process noise covariances. If coupled to an optimal command for the higher-order modes, then a globally optimal controller is achieved. It is only in *incomplete-information*

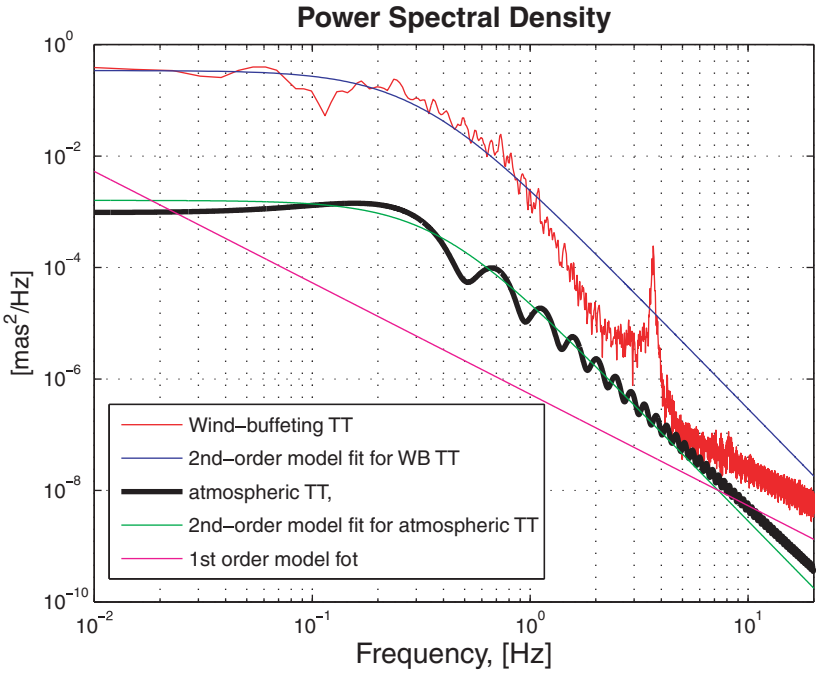

Fig. 4. Comparison of the temporal PSD of the atmospheric TT to the temporal PSD of wind-induced TT on the E-ELT M4-M5. Spectra obtained with the following custom parameters: D = 42 m, seeing = 1.1 mas@0.5 μm, thus $r_0 \approx 0.1$ m, a constant outer scale of turbulence $L_0 = 50$ m, with three-layers of turbulence profile with relative weights $\{0.67, 0.22, 0.11\}$, average wind speed $V_w = 12.5$ m/s and directions $\theta_i = \{0°, 45°, 90°\}$.

that using a TT-only controller lacks optimality by discarding TT correlations with higher-order modes sensed by the Hartmann-Shack, an inherent feature of the Kalman filter. Considering the amplitude of the correlations and the disparity of TT variance (about 90% of the total atmospheric turbulence) [21], this should represent a relatively small effect. To re-establish the globally optimal command, one can estimate via a Kalman filter the contribution of higher-order modes to the TT and feed it to the DM (that is itself also able to produce TT) to subtract it out. The controller structure is hence perfectly decoupled, with separate controllers for the TT and for the higher-modes. It has not been evaluated here and is left for future work.

Fig. 4 shows the temporal PSD of the atmospheric and wind-induced tip/tilt, obtained from a FEM simulation for the European ELT provided by ESO [29]. The fitted models are also shown to provide a more insightful interpretation. Wind-buffeting total variance is ≈280 mas rms to compare to ≈21 mas rms from the theoretical atmospheric tip/tilt [3]. This represents a ratio of more than two orders of magnitude in variance, which suggests that the bulk of the disturbance is from mechanical origin. The illustration given hereafter focuses therefore on compensating for wind-buffeting disturbances.

The work of [11] evidences the resonant behaviour of the E-ELT quaternary deformable mirror, that is taken as the applicative example of interest. These authors propose a second order model with a damping factor $\xi \approx 0.01$ and a resonant frequency that varies on a scale of 70–250 Hz. MV control for simpler models of the first order was addressed in [5].

4.1. Sample Numerical Results

The second order state-space model of Eqs (46) are used to model the tip/tilt behaviour of the E-ELT quaternary deformable mirror. This results in a DM model of the form (14), with

$$A_m = \begin{pmatrix} 0 & 1 \\ -\omega^2 & -2\omega\xi \end{pmatrix}, \tag{47a}$$

$$B_m = \begin{pmatrix} 0 \\ \omega^2 \end{pmatrix}, \tag{47b}$$

$$C_m = \begin{pmatrix} 1 & 0 \end{pmatrix}, \tag{47c}$$

$$D_m = 0, \tag{47d}$$

and $N = 1$.

Nominal values for the damping coefficient and natural frequency are $\xi = 0.01$ and $f_0 = 160$ Hz.

At the resonant frequency $f_r = f_0\sqrt{1-\xi^2}$, amplitude response is amplified by a factor of 50. This obviously configures a very weakly damped system that tends to oscillate at f_r with slow energy dissipation rate. So far

built finite-element models do not consider any supports that may considerably change these parameters (in either sense). They are used here only for illustration purposes. A broader discussion on large DM models can be found in [11].

The parameters of a continuous-time second order model of the tip/tilt turbulence mode have been fitted to the first points in the modal auto-correlation function. This function is computed from the power spectral density (PSD) using the Wiener-Khinchine theorem. The particular choice of parameters has been numerically validated in a robustness study presented in [7].

This model-fitting was performed for a telescope diameter of D = 42 m, with atmospheric seeing = 1.1 mas@0.5 μm, an outer scale of $L_0 = 50$ m and wind speed $V_w = 12.5$ m/s.

The resulting continuous-time stochastic turbulence model is defined by

$$A_\phi = \begin{pmatrix} -4.0 & -3.54 \\ 1 & 0 \end{pmatrix}, \tag{48a}$$

$$C_\phi = \begin{pmatrix} 0 & 3.54 \end{pmatrix}, \tag{48b}$$

with

$$\Sigma_\eta = \begin{pmatrix} 0.0213 & 0 \\ 0 & 0.059 \end{pmatrix}, \tag{49}$$

that guarantees $\Sigma_\phi = 0.0776\,\text{arcsec}^2$ of total disturbance variance.

The performance of the optimal solution and the solution that neglects the DM dynamics is compared in Fig. 5-left. It is clearly visible that the optimal solution guarantees the minimum residual variance (in milliarcseconds rms) throughout the resonant frequency range $f_0 \in [70, 250]$ Hz. Performance evaluations deduced from closed-loop covariance matrices (for the exact procedure refer to [7, 25]) show that a residual of about 3.5 mas rms is provided by the optimal regulator. These are to compare to values that vary between 4 and 9 mas rms within the stability region of the sub-optimal controller – reduced to the region [100–230] Hz. These results are backed by end-to-end temporal simulations that, for sake of clarity, are not discussed here but can be found in [7].

The variation of performance with respect to the damping coefficient is shown in Fig. 5-right. As expected, smaller damping coefficients (= greater amplitude resonant temporal responses) give rise to increased losses. For the optimal solution these do amount at no more than 0.02 mas rms whereas for the sub-optimal solution losses vary as much as 0.6 mas rms. Remarkably, the sub-optimal regulator is stable for $\xi \in [0.001, 0.1]$.

The improvement of the optimal over the sub-optimal solution (neglecting DM dynamics here) can be qualitatively appreciated by looking at the loop Bode plots. Fig. 6 depicts the rejection and noise transfer functions defined as

$$RTF(z) \triangleq \frac{\Phi^{\text{res}}(z)}{\Phi^{\text{tur}}(z)} = (1 + \mathscr{W}(z)\Gamma(z).\mathscr{M}(z))^{-1} \tag{50}$$

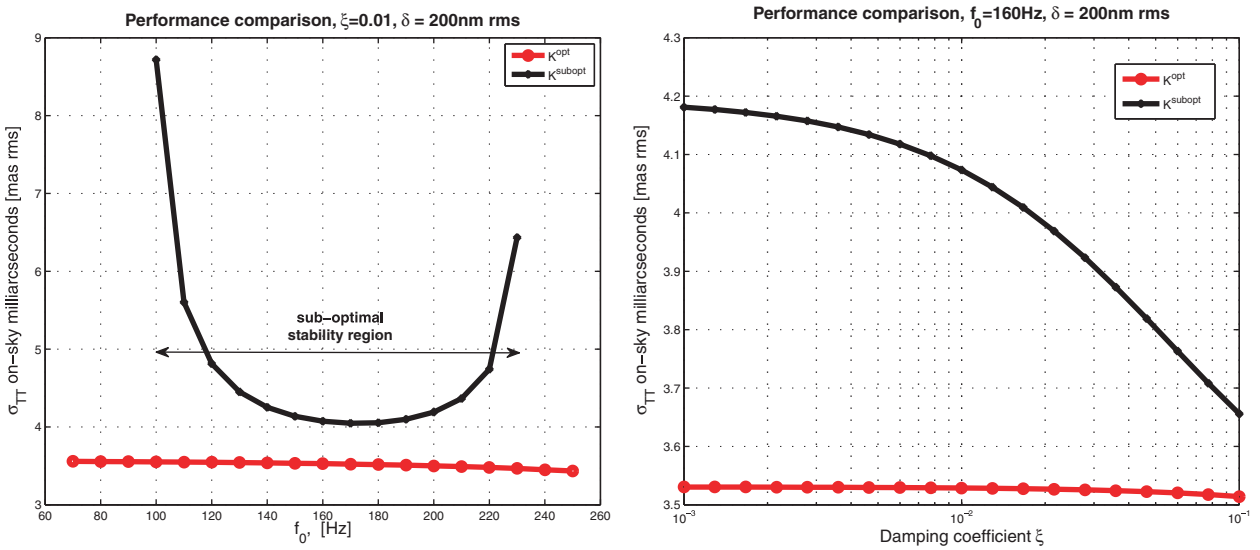

Fig. 5. Left: Performance comparison of the optimal and sub-optimal regulators. The double arrow indicates the stability region of the sub-optimal solution. Outside these bounds the sub-optimal regulator cannot operate. $T_s = 0.002s$, noise $\delta = 200$ nm rms at the edges of the telescope. Right: Performance comparison of the optimal and sub-optimal regulators. The sub-optimal regulator is found stable for all damping coefficients considered. $T_s = 0.002s$, noise $\delta = 200$ nm rms at the edges of the telescope.

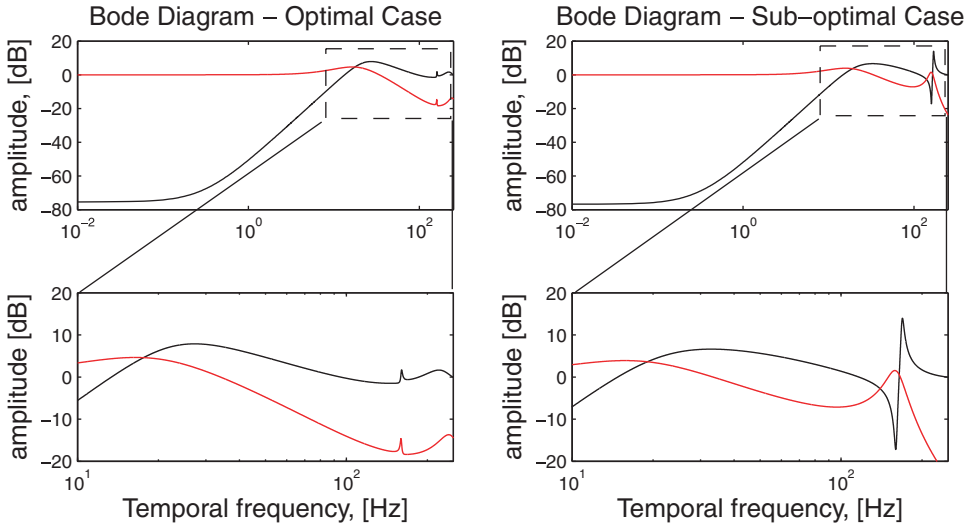

Fig. 6. Bode diagram comparison (amplitude only) for $f_0 = 160$ Hz, $\xi = 0.01$ and noise $\delta = 200$ nm rms at the edges of the telescope. Top panel: full diagram. Bottom panel: high-frequency zoom. Black/red curves for signal (RTF) and noise (NTF) rejection transfer functions.

and

$$NTF(z) \triangleq \frac{\Phi^{\mathrm{res}}(z)}{\mathsf{N}(z)} = \frac{\Gamma(z)\mathscr{M}(z)}{1 + \mathscr{W}(z)\Gamma(z)\mathscr{M}(z)} \tag{51}$$

where $\mathscr{W}(z)$, $\mathscr{M}(z)$ and $\Gamma(z)$ are respectively the WFS, the DM and the controller transfer functions.

In the optimal case, the resonant peak amplification is almost totally reduced by the controller rejection, providing better off-peak rejection for both the signal and noise. This grants a better balancing of the so-called water-bed effect, the resulting $\Phi^{\mathrm{res}}(z)$ being the flattest and smoothest in frequency.

The sub-optimal controller, being blind to the DM resonant peak, poorly rejects (actually it amplifies instead) both signal and noise around f_0 – see zoomed bottom panels in Fig. 6 – which is at the basis of the losses of performance presented in Fig. 5.

5. Summary

The LQG formulation proposed in this paper enables to compute the minimum variance AO controller and to evaluate the corresponding quadratic performance (residual phase variance), for a broad class of LTI DM dynamics models.

The benefits from taking into account DM dynamics in AO have been illustrated in the case of a tip-tilt mirror with resonant (second-order) dynamics. A markedly difference in performance is observed when the sub-optimal regulator gets close to its stability limits, which is considerably reduced to the [100–230] Hz.

Synthesis of optimal controllers and performance comparison and evaluation are specially useful at a time when several projects are either ongoing or in design stage to go from active to adaptive telescopes (*i.e.* where the optical path is itself adaptive) for they allow a better dimensioning. Adaptive telescopes require larger DMs and more complex structures to control. These include the deformable secondary (DSM) at ESO's Very Large Telescope (VLT), the M4-M5 unit at ESO's projected European-Extremely Large Telescope (E-ELT) , the NFIRAOS tip-tilt mount for the Thirty-Meter Telescope project (TMT) and the Large Binocular Telescope (LBT) deformable secondary to cite a few. Such DMs will likely present resonant frequencies and modal coupling (not addressed in this contribution). The formulation given here can incorporate such constraints to tackle both issues.

However, suitably characterised real-sized models of such systems are still largely unavailable, for they are still in the early phases of the design stages, with few test benches built so far. As noted, the control design tool presented herein can accommodate a fairly wide class of DM models. However, an important practical limitation of this approach is that both the DM and turbulent phase models are required to reproduce with sufficient accuracy the inter-sampling behaviour of both subsystems – clearly, an exacting challenge.

This LQG formulation also authorises other potentially interesting extensions. These include (1) coping with DM control penalisation, (2) optimal control of a two-DMs woofer-tweeter system and (3) asynchronous operation of the WFS and DM. Other topics for future investigation are robustness of stability/performance with respect to

models uncertainties/variations and on-line model identification.

Acknowledgements

The authors wish to acknowledge fruitful discussions with Dominique Le Bihan @ ONERA and Rami Gasmi @ Obs. Paris-Meudon on the DM dynamical models; the European Southern Observatory in the person of B. Sedghi for providing the wind-shake data.

This work was partially funded by FCT under contract number SFRH/BD/30010/2006 and by French National Agency through project CHAPERSOA ANR-09-BLAN-0162-01.

References

1. Anderson BDO, Moore JB. *Optimal Filtering*. Dover Publications Inc., 1995.
2. Arsenault R, Biasi R, Gallieni D, Riccardi A, Lazzarini P, Hubin N, Fedrigo E, Donaldson R, Oberti S, Stroebele S, Conzelmann R, Duchateau M. A deformable secondary mirror for the VLT. In Ellerbroek BL, Calia DB (eds.). *Proceedings of the SPIE*, *SPIE* 2006; 6272, p. 62720V.
3. Conan J-M, Rousset G, Madec P-Y. Wave-front temporal spectra in high-resolution imaging through turbulence. *J Opt Soc Am A* 1995; 12: 1559–1570.
4. Correia C, Conan J-M, Kulcsár C, Raynaud H-F, Petit C. Adapting optimal LQG methods to ELT-sized AO systems. In *Proceeding of the AO4ELT Conference*. EDP Sciences, 2009.
5. Correia C, Kulcsár C, Conan J-M, Raynaud H-F. Hartmann modelling in the discrete spatial-frequency domain: application to real-time reconstruction in adaptive optics. In Hubin N, Max CE, Wizinowich PL (eds.). *Proceedings of the SPIE*, *SPIE* 2008; 7015, p. 701551.
6. Correia C, Raynaud H-F, Kulcsár C, Conan J-M. Accounting for mirror dynamics in optimal adaptive optics control. In *Proceedings of the European Control Conference*, 2009.
7. Correia C, Raynaud H-F, Kulcsár C, Conan J-M. On the optimal reconstruction and control of adaptive optical systems with mirroir dynamics. *J Opt Soc Am A* 2010; 27(2): 333–349.
8. Costille A, Petit C, Conan J-M, Kulcsár C, Raynaud H-F, Fusco T. Wide field adaptive optics laboratory demonstration with closed loop tomographic control. *J Opt Soc Am A* 2010; 27(3): 469–483.
9. Dessenne C, Madec P-Y, Rousset G. Sky implementation of modal predictive control in adaptive optics. *Opt Lett* 1999; 24(5): 339–341.
10. Fusco T, Conan J-M, Rousset G, Mugnier LM, Michau V. Optimal wave-front reconstruction strategies for multiconjugate adaptive optics. *J Opt Soc Am A* 2001; 18: 2527–2538.
11. Gasmi R, Sinquin JC, Jagourel P, Dournaux JL, Le Bihan D, Hammer F. Modeling of a large deformable mirror for future E-ELT. In *Proceedings of the SPIE*, 2008; 7017.
12. Gendron E, Léna P. Astronomical adaptive optics I: Modal control optimization. *Astron Astrophys* 1994; 291: 337–347.
13. Herrmann J. Phase variance and Strehl ratio in adaptive optics. *J Opt Soc Am A* 1992; 9: 2257–2258.
14. Hinnen K, Verhaegen M, Doelman N. Exploiting the spatiotemporal correlation in adaptive optics using data-driven *H*2-optimal control. *J Opt Soc Am A* 2007; 24: 1714–1725.
15. Hardy JW. *Adaptive Optics for Astronomical Telescopes*. Oxford, New York, 1998.
16. Kulcsár C, Raynaud H-F, Petit C, Conan J-M. Optimal ao control with ngs/lgs wavefront sensors: the multirate case. *SPIE* 2010; 7736: p. 773614.
17. Kulcsár C, Raynaud H-F, Petit C, Conan J-M, de Lesegno PV. Optimal control, observers and integrators in adaptive optics. *Opt Express* 2006; 14(17): 7464–7476.
18. Le Roux B, Conan J-M, Kulcsár C, Raynaud H-F, Mugnier LM, Fusco T. Optimal control law for classical and multiconjugate adaptive optics. *J Opt Soc Am A* 2004; 21: 1261–1276.
19. Looze DP. Discrete-time model of an adaptive optics systems. *J Opt Soc Am A* 2007; 24: 2850–2863.
20. Looze DP. Linear-quadratic-gaussian control for adaptive optics systems using a hybrid model. *J Opt Soc Am A* 2009; 26(1): 1–9.
21. Noll RJ. Zernike polynomials and atmospheric turbulence. *J Opt Soc Am A* 1976; 66: 207–211.
22. Paschall R, Von Bokern M, Welsh B. Design of a linear quadratic Gaussian controller for an adaptive optics system. In *Proceedings of the 30th IEEE Conference on Decision and Control*, 1991; 2: 1761–1769.
23. Paschall RN, Anderson DJ. Linear Quadratic Gaussian control of a deformable mirror adaptive optics system with time-delayed measurements. *Appl Opt* 1993; 32: 6347–6358.
24. Petit C, Conan J-M, Kulcsár C, Raynaud H-F. Linear quadratic gaussian control for adaptive optics and multiconjugate adaptive optics: experimental and numerical analysis. *J Opt Soc Am A* 2009; 26(6): 1307–1325.
25. Raynaud H-F, Correia C, Kulcsár C, Conan J-M. Minimum-variance control of astronomical adaptive optics systems with actuator dynamics under synchronous and asynchronous sampling. *Int J Robust Nonlinear Control*, 2010; 21(7): 768–789.
26. Riccardi A, Xompero M, Zanotti D, Busoni L, Del Vecchio C, Salinari P, Ranfagni P, Brusa Zappellini G, Biasi R, Andrighettoni M, Gallieni D, Anaclerio E, Martin HM, Miller SM. The adaptive secondary mirror for the Large Binocular Telescope: results of acceptance laboratory test. In *Proceedings of the SPIE*, 2008, p. 7015.
27. Roddier F. *Adaptive Optics in Astronomy*. Cambridge University Press, New York, NY: Cambridge University Press, 1999.
28. Rousset G, Fontanella JC, Kern P, Gigan P, Rigaut F. First diffraction-limited astronomical images with adaptive optics. *Astron Astrophys* 1990; 230: L29–L32.
29. Sedghi B. E-ELT Main Axis Control Analysis, Issue 3. Technical report, European Southern Observatory, 2007.
30. Wiberg DM, Max CE, Gavel DT. A spatial non-dynamic LQG controller part I, application to adaptive optics. In *43rd IEEE Conference on Decision and Control, 2004. CDC* 1994, p. 3.

Appendix A: Details of proof for Proposition 1

From $\phi^{\text{cor}}(t) = Np(t)$, we get at any time t

$$\left\|\phi^{\text{res}}(t)\right\|^2 = \left\|\phi^{\text{tur}}(t)\right\|^2 - 2p(t)^{\text{T}} N^{\text{T}} \phi^{\text{tur}}(t) + p(t)^{\text{T}} N^{\text{T}} Np(t). \tag{52}$$

Denote as F the transfer function from u to p, *i.e.* $F(\mathbf{s}) = C_m(\mathbf{s}I - A_m)^{-1} B_m + D_m$. With a unitary DC gain, $F(0) = D_m - C_m A_m^{-1} B_m = I$. Using (24) and the identity $\int_0^s e^{vA_m} dv = A_m^{-1}\left(e^{sA_m} - I\right)$, we get

$$p(nT_s + s) = C_m e^{sA_m} x_n^m + \left(I + C_m e^{sA_m} A_m^{-1} B_m\right) u_n, \tag{53}$$

$$\frac{1}{T_s}\int_{nT_s}^{(n+1)T_s} p(t)^T N^T Np(t)\, dt = \left(x_n^m\right)^T Q_0 x_n^m + 2\left(x_n^m\right)^T S_0 u_n + u_n^T R_1 u_n; \tag{54}$$

$$\frac{1}{T_s}\int_{nT_s}^{(n+1)T_s} p(t)^T N^T \phi^{\text{tur}}(t)\, dt = u_n^T N^T \overline{\phi}_{n+1}^{\text{tur}} + \left(x_{m,n} + A_m^{-1} B_m u_n\right)^T \overline{\varphi}_{n+1}^{\text{tur}}. \tag{55}$$

This shows that $j_n^{\text{c}}(u)$ can be expressed as

$$j_n^{\text{c}}(u) = z_n^T Q_1 z_n + 2 z_n^T S_1 u_n + u_n^T R_1 u_n, \tag{56}$$

with

$$Q_1 \triangleq \begin{pmatrix} 0 & 0 & 0 \\ 0 & 0 & -I \\ 0 & -I & Q_0 \end{pmatrix}. \tag{57}$$

Since (54) is the integral of a non-negative function, so is the associated quadratic form:

$$P_0 \triangleq \begin{pmatrix} Q_0 & S_0 \\ S_0^T & R_1 \end{pmatrix} \geq 0. \tag{58}$$

Suppose that (54) is zero for some (z_n, u_n). Since $N^T N$ is invertible and p is a continuous function over $[nT_s, (n+1)T_s]$, it follows that $p(t)$ is everywhere zero on this interval, and thus that all its right-derivatives at $t = nT_s$ are also zero:

$$p_n = p(nT_s) = C_m x_n^m + D_m u_n = 0, \tag{59}$$

$$\forall i > 0, \quad \frac{d^i p}{dt^i}(nT_s) = C_m A_m^i x_n^m + C_m A_m^{i-1} B_m u_n = 0. \tag{60}$$

This last identity means that for all $i \geq 0$, $A_m x_{m,n} + B_m u_n \in \ker\left(C_m A_m^i\right)$, in other words that $A_m x_m^m + B_m u_n$ is an unobservable initial condition for (A_m, C_m). Since (A_m, C_m) is observable, $A_m x_n^m + B_m u_n = 0$, so that (x_n, u_n) is an equilibrium point of Eq. (14). Because the DC gain between u and p is unitary, this equilibrium point verifies $C_m x_{m,n} + D_m u_n = u_n = 0$. It follows that $x_{m,n}$ is also an unobservable initial condition for (A_m, C_m), and thus that $(x_n, u_n) = 0$. This establishes that $P_0 > 0$.

Finally, because $P_0 > 0$, one can find $\kappa > 0$ such that $P_0 > (1/\kappa)I$. It is easily checked that adding suitable diagonal terms in Q1 results in $Q_2 \geq 0$ and $P \geq 0$, which completes the proof.

Appendix B: Analytical performance evaluation

Using Propositions 1 and 2, the globally optimal MV control is obtained as the solution of a standard discrete-time LQG problem, *i.e.* as $u_n^{ii} = -K_\infty \widehat{x}_{n|n-1}$, where $\widehat{x}_{n|n-1}$ is the output of a stationary Kalman filter in prediction form:

$$\widehat{x}_{n|n-1} = A\widehat{x}_{n-1|n-2} + Bu_{n-1} + L_\infty\left(q_{n-1} - C\widehat{x}_{n-1|n-2}\right). \tag{61}$$

Note that the optimal control/observer gains K_∞, L_∞ can be computed as the solutions of reduced-order ARE, since the corresponding MV control/prediction sub-problems each mobilise only part of the state vector x (e.g. the value of delayed inputs need not be estimated, while the optimal observer gain for the DM state is necessarily zero, since the DM model is noiseless).

The model can also be used to directly evaluate the value of the original performance criterion J^{c} for both the MV control or any sub-optimal reconstructed feedback. This follows from identity

$$J^{\text{c}}(u) = \lim_{T_f \to +\infty} \frac{1}{T_f}\int_0^{T_f} \left\|\phi^{\text{tur}}(t)\right\|^2 dt + \lim_{M \to +\infty} \frac{1}{M}\sum_{n=0}^{M-1}\left(z_n^T Q_1 z_n + 2 z_n^T S_1 u_n + u_n^T R_1 u_n\right). \tag{62}$$

Since ϕ^{tur} is an ergodic process, $\text{E}(\cdot)$ denoting expectation, we get *almost surely* (a.s.)

$$\lim_{T_f \to +\infty} \frac{1}{T_f}\int_0^{T_f} \left\|\phi^{\text{tur}}(t)\right\|^2 dt \overset{a.s.}{=} \text{E}\left(\left\|\phi^{\text{tur}}(t)\right\|^2\right), \tag{63}$$

at any time t, including sampling instants $t = nT_s$. Thus,

$$\lim_{T_f \to +\infty} \frac{1}{T_f} \int_0^{T_f} \left\| \phi^{\text{tur}}(t) \right\|^2 dt \overset{a.s.}{=} \text{trace}\left(C'_\phi C'^T_\phi \Sigma_\infty \right), \tag{64}$$

where $C'_\phi \triangleq \begin{pmatrix} C_\phi & \cdots & 0 & 0 \end{pmatrix}$ and Σ_∞ is the steady-state closed-loop covariance matrix for the augmented state $[x^T, \hat{x}^T_{n|n-1}]^T$, *i.e.* the solution of the discrete Lyapunov equation $\Sigma_f = A_f \Sigma_f A_f^T + \Sigma'$, with

$$A_f \triangleq \begin{pmatrix} A & -BK_\infty \\ L_\infty C & A - BK_\infty - L_\infty C \end{pmatrix}, \tag{65}$$

$$\Sigma' \triangleq \begin{pmatrix} \Gamma \Sigma_v \Gamma^T & 0 \\ 0 & L_\infty \Sigma_w L_\infty^T \end{pmatrix}. \tag{66}$$

Thus, for any optimal or sub-optimal choice of K_∞, L_∞ (on the assumption they stabilise the loop), it is immediately checked that

$$J^{\text{c}}(u) \overset{a.s.}{=} \text{trace}\left(Q \Sigma_f \right), \tag{67}$$

where

$$Q \triangleq \begin{pmatrix} C'_\phi C'^T_\phi + G^T Q_1 G & K_\infty^T S_1^T G \\ G^T S_1 K_\infty & K_\infty^T R_1 K_\infty \end{pmatrix}. \tag{68}$$

The construction results mostly from routine application of standard discretization formulae.